

## Spin correlations in spin blockade

To cite this article: Rafael Sánchez *et al* 2008 *New J. Phys.* **10** 115013

View the [article online](#) for updates and enhancements.

### Related content

- [Semiconductor quantum dots for electron spin qubits](#)  
W G van der Wiel, M Stopa, T Kodera *et al.*
- [Dynamical nuclear spin polarization induced by electronic current through double quantum dots](#)  
Carlos López-Monís, Jesús Iñarrea and Gloria Platero
- [Time-dependent single-electron transport](#)  
Toshimasa Fujisawa, Toshiaki Hayashi and Satoshi Sasaki

### Recent citations

- [Photon assisted long-range tunneling](#)  
Fernando Gallego-Marcos *et al*
- [Steady-State Coherent Transfer by Adiabatic Passage](#)  
Jan Huneke *et al*
- [Correlations of heat and charge currents in quantum-dot thermoelectric engines](#)  
Rafael Sánchez *et al*

## Spin correlations in spin blockade

Rafael Sánchez<sup>1</sup>, Sigmund Kohler<sup>2</sup> and Gloria Platero<sup>1,3</sup>

<sup>1</sup> Instituto de Ciencia de Materiales de Madrid (CSIC), Cantoblanco, 28049 Madrid, Spain

<sup>2</sup> Institut für Physik, Universität Augsburg, Universitätstraße 1, 86135 Augsburg, Germany

E-mail: [gloria.platero@icmm.csic.es](mailto:gloria.platero@icmm.csic.es)

*New Journal of Physics* **10** (2008) 115013 (16pp)

Received 26 June 2008

Published 20 November 2008

Online at <http://www.njp.org/>

doi:10.1088/1367-2630/10/11/115013

**Abstract.** We investigate spin currents and spin-current correlations for double quantum dots in the spin blockade regime. By analysing the time evolution of the density matrix, we obtain the spin resolved currents and derive from a generating function an expression for the fluctuations and correlations. Both the charge current and the spin current turn out to be generally super-Poissonian. Moreover, we study the influence of ac fields acting upon the transported electrons. In particular, we focus on fields that cause spin rotation or photon-assisted tunnelling.

<sup>3</sup> Author to whom any correspondence should be addressed.

**Contents**

<b>1. Introduction</b>	<b>2</b>
<b>2. Model and method</b>	<b>3</b>
2.1. Master equation and full counting statistics . . . . .	4
2.2. Stationary solution and zero-frequency noise . . . . .	5
2.3. Spin current fluctuations . . . . .	6
<b>3. Spin current noise for undriven quantum dots</b>	<b>6</b>
<b>4. Electron spin resonance</b>	<b>8</b>
4.1. Crossover to the incoherent regime: unblocking by relaxation . . . . .	10
<b>5. Pumping and photon-assisted transport</b>	<b>11</b>
<b>6. Conclusions</b>	<b>14</b>
<b>Acknowledgments</b>	<b>15</b>
<b>References</b>	<b>15</b>

**1. Introduction**

The recently achieved access to individual electron states of quantum dots [1] spurred the interest in the control of single electron degrees of freedom in nanoconductors providing a designable alternative to atoms in quantum optics. In particular, by applying ac fields, interesting effects such as coherent destruction of electron tunnelling by electric ac fields [2]–[7] or electron spin rotations by crossed magnetic ac and dc fields [8]–[10] have been reported. A double quantum dot with up to two electrons provides a perfect framework for spin manipulation via *spin blockade* [11]–[14]. These systems are designed such that the only state located in the transport window is the doubly occupied singlet state. In this particular configuration, for electrons occupying inter-dot triplet states, i.e. two-electron states in which the electrons have the same spin orientation, inter-dot tunnelling is suppressed due to the Pauli exclusion principle. Tunnelling current in ac electric fields [4], [15]–[17] can be tuned by means of the frequency and intensity of the field, which yields interesting features like for instance charge localization within the quantum dot structure (dynamical localization) and suspension of Coulomb and spin blockade.

Spin blockade also plays an important role for coherent spin manipulation, as demonstrated by electron spin resonance experiments where a resonant ac magnetic field—perpendicular to a dc one—acts on the double quantum dot [9] giving rise to coherent single-spin rotations. Under certain configurations, the singlet states are populated such that spin blockade is lifted and, thus, an electronic current flows through the system. Then the current exhibits signatures of an interplay between coherent spin rotations due to the ac magnetic field and coherent electron delocalization due to interdot tunnelling [10].

In this paper, we analyse the spin current and the spin current fluctuations, as well as their correlations in double quantum dots in the spin blockade regime in the presence of ac-electric and magnetic fields. We demonstrate that spin current correlations provide information about the spin dynamics. Moreover, we also consider the case of spin relaxation which stems from spin flip processes accompanied by the coupling to a bosonic heat bath. This heat bath together with the fermionic electron reservoirs forms an unconventional environment for the quantum dots.

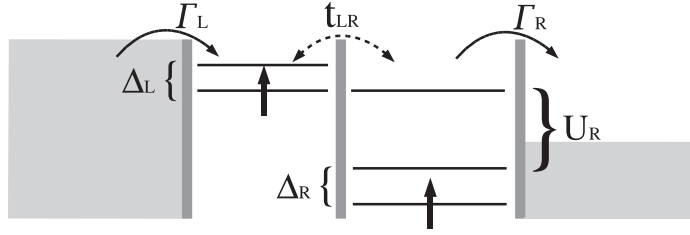


**Figure 1.** Double quantum dot in spin blockade configuration. The chemical potentials in the contacts are adjusted such that the doubly occupied intra-dot singlet state is the only one located in the transport window. As electrons fall in the inter-dot triplet subspace, inter-dot tunnelling is forbidden by spin conservation. Consequently, transport is suppressed.

## 2. Model and method

We consider two weakly coupled quantum dots connected to two fermionic leads (cf figure 1) described by the Hamiltonian

$$\hat{H} = \hat{H}_0 + \hat{H}_{LR} + \hat{H}_T + \hat{H}_{\text{leads}}, \quad (1)$$

where  $\hat{H}_0 = \sum_{i\sigma} \varepsilon_{i\sigma} \hat{c}_{i\sigma}^\dagger \hat{c}_{i\sigma} + \sum_i U_i \hat{n}_{i\uparrow} \hat{n}_{i\downarrow} + U_{LR} \hat{n}_L \hat{n}_R$  describes the two isolated quantum dots,  $\hat{H}_{LR} = -\sum_{\sigma} (t_{LR} \hat{c}_{L\sigma}^\dagger \hat{c}_{R\sigma} + \text{h.c.})$  is the inter-dot coupling.  $\hat{H}_T = \sum_{l \in \{L,R\}k\sigma} (\gamma_l \hat{d}_{lk\sigma}^\dagger \hat{c}_{l\sigma} + \text{h.c.})$  represents the tunnelling between the double quantum dot and the leads described by  $\hat{H}_{\text{leads}} = \sum_{lk\sigma} \varepsilon_{lk\sigma} \hat{d}_{lk\sigma}^\dagger \hat{d}_{lk\sigma}$ .  $\varepsilon_{i\sigma}$  is the energy of an electron located in dot  $i$  with spin  $\sigma$ , and  $U_i$  ( $U_{LR}$ ) is the intra-dot (inter-dot) Coulomb repulsion. In order to allow for up to two electrons in the system (one in each dot), the chemical potentials of the leads,  $\mu_i$ , must satisfy the condition  $\varepsilon_i < \mu_i - U_{LR} < \varepsilon_i + U_i$  and  $\mu_i < \varepsilon_i + 2U_{LR}$ . In addition, a dc-magnetic field is introduced along the  $z$ -axis in order to break the spin degeneracy by a Zeeman splitting  $\Delta_i = g_i B_{z,i}$ , i.e.  $\hat{H}_B = \sum_i \Delta_i \hat{S}_z^i$ , where  $\mathbf{S}_i = \frac{1}{2} \sum_{\sigma\sigma'} c_{i\sigma}^\dagger \boldsymbol{\sigma}_{\sigma\sigma'} c_{i\sigma'}$  are the spin operators of each dot.

In this configuration, spin blockade is manifest for sufficiently small bias voltage such that the state with two electrons in the right dot (the state that supports the current) is in resonance with the one electron states in each dot. The current is then quenched whenever the electrons in each quantum dot have the same spin polarization and the Pauli exclusion principle avoids inter-dot tunnelling [12].

Moreover, considering that any excited state in the right quantum dot has an energy above the transport window and that inter-dot tunnelling is spin independent, a current can flow only through processes involving the doubly occupied singlet in the right quantum dot,  $|S_R\rangle$  and the inter-dot singlet  $|S_0\rangle = (|\uparrow, \downarrow\rangle - |\downarrow, \uparrow\rangle)/\sqrt{2}$ . Thus, the occupation of any inter-dot triplet state,  $|+\rangle = |\uparrow, \uparrow\rangle$ ,  $|-\rangle = |\downarrow, \downarrow\rangle$  and  $|T_0\rangle = (|\uparrow, \downarrow\rangle + |\downarrow, \uparrow\rangle)/\sqrt{2}$  inhibits the transport to the collector [10], unless, as we will discuss below, the singlet and the triplet subspace mix due to any perturbation, as for instance an inhomogeneous magnetic field in the sample, which produces different Zeeman splittings within each quantum dot.

### 2.1. Master equation and full counting statistics

The non-equilibrium dynamics of a quantum dot system can be described by means of the equation of motion for the reduced density operator  $\rho$ , obtained after tracing out the reservoirs in the total density operator  $R$ :

$$\dot{\rho} = \text{tr}_{\mathcal{R}} \dot{R} = -\frac{i}{\hbar} \text{tr}_{\mathcal{R}} [H, R] = \mathcal{L}\rho, \quad (2)$$

where  $\mathcal{L}$  is the Liouvillian acting on the reduced density operator. In matrix notation, it reads  $\dot{\rho}_i = \mathcal{M}_{ij}\rho_j$ , where  $\rho_j$  denotes the density operator in vector notation.

Accordingly, one can define current super-operators  $\mathcal{J}_{\pm}$  which, when acting on the reduced density operator, describe the electron tunnelling from the quantum dots to the collector and back, thus yielding positive and negative contributions to the current. Then, the current can be formulated as the trace of the current operator [18, 19]

$$I = e \text{tr}_S(\mathcal{J}\rho) = e \text{tr}_S[(\mathcal{J}_+ - \mathcal{J}_-)\rho]. \quad (3)$$

Note that, in the same way as the super-operator  $\mathcal{L}$  can be written as a matrix and  $\rho$  as a vector, the trace over the system space can be expressed as multiplication with a transposed vector in Liouvillian space,  $v_0^\dagger$ , which is the unit matrix in vector notation. Thus, the trace condition  $\text{tr}_S \rho = 1$  reads  $v_0^\dagger \rho = 1$ , while trace conservation  $\text{tr}_S \dot{\rho} = 0$  corresponds to the relation

$$v_0^\dagger \mathcal{L} = 0 \quad (4)$$

and the current expectation value becomes  $I = e v_0^\dagger \mathcal{J}\rho$ .

It is convenient to write the master equation with the help of the current operators, which is easily done by identifying those terms that change the number of particles in the collector included in  $\mathcal{J}_{\pm}$ . Then the master equation assumes the form

$$\dot{\rho} = \mathcal{L}(t)\rho = (\mathcal{L}_0(t) + \mathcal{J}_+ + \mathcal{J}_-)\rho. \quad (5)$$

In a quantum dot system, the super-operator  $\mathcal{L}_0(t)$  describes both the electron dynamics and tunnelling through the emitter barrier.

Both current and shot noise can be expressed in terms of the accumulated charge in the collector,  $eN(t)$ , such that [20]

$$I = e \frac{d}{dt} \langle N(t) \rangle, \quad (6)$$

$$S = e^2 \frac{d}{dt} (\langle N^2(t) \rangle - \langle N(t) \rangle^2). \quad (7)$$

Accordingly, one can obtain expressions for the higher order moments of the current by evaluating the expectation value  $\langle N^\alpha \rangle$ ,  $\alpha = 1, 2, 3, \dots$ , that define the statistics of the transmitted electrons—the *full counting statistics* [21, 22].

For the specific computation of the cumulants, we define the operator

$$G(z, t) = \text{tr}_{\mathcal{R}} (z^N R(t)), \quad (8)$$

which generalizes the density operator. The latter is recovered in the limit  $G(z \rightarrow 1, t) = \text{tr}_{\mathcal{R}} R(t) = \rho(t)$ .  $G(z, t)$  obeys the equation of motion

$$\dot{G}(z, t) = (\mathcal{L} + (z - 1)\mathcal{J}_+ + (z^{-1} - 1)\mathcal{J}_-) G(z, t), \quad (9)$$

whereas its trace is the moment generating function for the transported electrons, which means

$$\langle N^\alpha \rangle = v_0^\dagger \left( z \frac{\partial}{\partial z} \right)^\alpha G(z, t) \Big|_{z=1} \equiv \text{tr}_S g^{(\alpha)}(t), \quad (10)$$

where

$$g^{(\alpha)}(t) = \left( z \frac{\partial}{\partial z} \right)^\alpha G(z, t) \Big|_{z=1} = \text{tr}_R (N^\alpha R(t)). \quad (11)$$

Introducing the shorthand notation  $g \equiv g^{(0)}$  and  $g' \equiv g^{(1)}$ , we find the equations of motion [19]

$$\dot{g}(t) = \dot{\rho}(t) = \mathcal{L}\rho(t), \quad (12)$$

$$\dot{g}'(t) = \mathcal{L}g'(t) + (\mathcal{J}_+ - \mathcal{J}_-)\rho(t). \quad (13)$$

The corresponding equations of motion for the higher order moments allow the recursive computation of the full counting statistics without the need of explicitly computing eigenfunctions and derivatives [23]. This is particularly helpful for larger systems that require a numerical treatment.

## 2.2. Stationary solution and zero-frequency noise

The average current and the shot noise can be obtained by integrating the equations of motion (12) and (13). For long times, the system evolves into a stationary state determined by  $\mathcal{L}\rho_\infty = 0$ . The stationary solution  $\rho_\infty$  thus is the eigenvector of the Liouvillian that corresponds to the eigenvalue zero with the normalization  $v_0^\dagger \rho_\infty = 1$ . By inserting this into equation (13), we obtain

$$\dot{g}'(t) = \mathcal{L}g'(t) + (\mathcal{J}_+ - \mathcal{J}_-)\rho_\infty. \quad (14)$$

The eigenvalue zero of  $\mathcal{L}$ , which corresponds to the stationary state, involves a solution with one component linear in time, which can be singled out by projection to the null-space,  $\rho_\infty v_0^\dagger$ , such that

$$g'(t) = \rho_\infty v_0^\dagger (\mathcal{J}_+ - \mathcal{J}_-) \rho_\infty t + g'_\perp(t). \quad (15)$$

The orthogonal component  $g'_\perp(t)$ , converges for long times, as we will demonstrate below. The information about the shot noise is fully contained in  $g'_\perp(t)$ , and for its stationary solution, we obtain by inserting (15) into (13) the algebraic equation

$$\mathcal{L}g'_\perp(\infty) = (\rho_\infty v_0^\dagger - 1)(\mathcal{J}_+ - \mathcal{J}_-)\rho_\infty, \quad (16)$$

together with the orthogonality condition  $v_0^\dagger g'_\perp(\infty) = 0$ . The numerical integration of equations (12) and (13), as well as the projection to the orthogonal subspace are illustrated in figure 2.

Knowing  $\rho_\infty$  and  $g'_\perp(\infty)$  allows one to compute the stationary current and the zero-frequency noise

$$I = e v_0^\dagger (\mathcal{J}_+ - \mathcal{J}_-) \rho_\infty \quad (17)$$

$$S = e^2 v_0^\dagger \{ (\mathcal{J}_+ - \mathcal{J}_-) g'_\perp(\infty) + (\mathcal{J}_+ + \mathcal{J}_-) \rho_\infty \}, \quad (18)$$

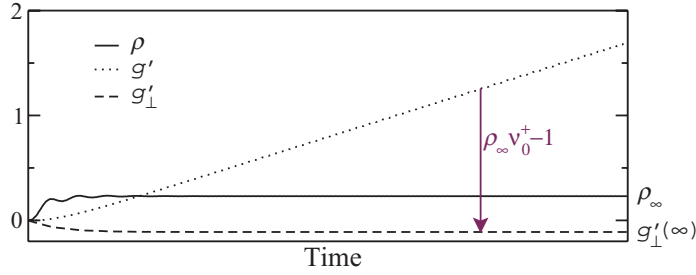


**Figure 2.** Time evolution of a typical diagonal element of the density matrix  $\rho$  and the corresponding terms of  $g'$  and  $g'_{\perp}$ , see section 2.2.

respectively. The ratio between them defines the Fano factor

$$F = \frac{S}{e|I|}, \quad (19)$$

which reflects the sub- or super-Poissonian character of the noise according to  $F < 1$  or  $F > 1$ , respectively. This method is also valid for ac-driven systems provided that one considers the averages  $\bar{I}$  and  $\bar{S}$  over one period of the field [19].

### 2.3. Spin current fluctuations

Up to now we considered the statistics of the *total* transferred charge. However, we are also interested in the spin degree of freedom and the eventual spin–spin correlations. It is straightforward to adapt the formalism presented above to the case of transport of electrons with spin  $\sigma = \uparrow, \downarrow$  by replacing in equations (6) and (7) the electron number operator,  $N$ , by number operator for electrons with spin  $\sigma = \uparrow, \downarrow$ ,  $N_{\sigma}$ . Then one obtains the spin current operators  $\mathcal{J}_{\sigma\pm}$  and the corresponding spin currents  $I_{\sigma} = e \frac{d}{dt} \langle N_{\sigma} \rangle$ , as well as the spin auto-correlation  $S_{\sigma} = e^2 \frac{d}{dt} (\langle N_{\sigma}^2 \rangle - \langle N_{\sigma} \rangle^2)$  with the spin Fano factor  $F_{\sigma} = S_{\sigma} / (e|I_{\sigma}|)$ .

Moreover, by comparing charge noise and spin noise, one can also study cross-correlations of currents with opposite spin whose zero-frequency component reads

$$S_{\uparrow\downarrow} = \frac{d}{dt} (\langle N_{\uparrow} N_{\downarrow} \rangle - \langle N_{\uparrow} \rangle \langle N_{\downarrow} \rangle) = \frac{1}{2} (S - \sum_{\sigma=\uparrow,\downarrow} S_{\sigma}). \quad (20)$$

This quantity allows one to define the dimensionless spin correlation coefficient

$$r = \frac{S_{\uparrow\downarrow}}{\sqrt{S_{\uparrow} S_{\downarrow}}}, \quad (21)$$

which assumes the value  $r = 1$ , if the transport of  $\uparrow$ -electrons and  $\downarrow$ -electrons is perfectly correlated, whereas  $r = 0$  for uncorrelated spin currents.

## 3. Spin current noise for undriven quantum dots

In the configuration described in section 2, i.e. for two quantum dots with up to two electrons in the system, it is convenient to decompose the density operator into the basis  $|1\rangle = |0, \uparrow\rangle$ ,  $|2\rangle = |0, \downarrow\rangle$ ,  $|a\rangle = |\uparrow, \downarrow\rangle$ ,  $|b\rangle = |\downarrow, \uparrow\rangle$ ,  $|S_R\rangle = |0, \uparrow\downarrow\rangle$ ,  $|+\rangle = |\uparrow, \uparrow\rangle$  and  $|-\rangle = |\downarrow, \downarrow\rangle$ . As discussed above, transport suffers from spin blockade unless the inter-dot triplet states have finite lifetime.

However, as discussed in [24], transport becomes possible for a small but finite thermal smearing of the Fermi surface of the emitter. Then an electron in the left quantum dot being in one of the states  $|a\rangle$ ,  $|b\rangle$ ,  $|\pm\rangle$  can tunnel with a rate  $x\Gamma_L$  to the emitter, where  $x = 1 - f(\varepsilon_L + U_{LR})$ , and can be replaced by an electron with opposite spin. We neglect here the contribution of leakage currents due to co-tunnelling [25, 26].

Under the usual Born–Markov approximation [27], the master equation for the reduced density matrix,  $\dot{\rho} = \mathcal{L}\rho$ , in presence of an homogeneous magnetic field, i.e. for  $\Delta_L = \Delta_R$  reads

$$\begin{aligned}
\dot{\rho}_1 &= \Gamma_R \rho_{S_R} + x\Gamma_L(\rho_b + \rho_+) - 2(1-x)\rho_1, \\
\dot{\rho}_2 &= \Gamma_R \rho_{S_R} + x\Gamma_L(\rho_a + \rho_-) - 2(1-x)\rho_2, \\
\dot{\rho}_a &= -2t_{LR} \text{Im} \rho_{S_R a} - x\Gamma_L \rho_a + (1-x)\Gamma_L \rho_1, \\
\dot{\rho}_b &= 2t_{LR} \text{Im} \rho_{S_R b} - x\Gamma_L \rho_b + (1-x)\Gamma_L \rho_1, \\
\dot{\rho}_{S_R} &= 2t_{LR} \text{Im}(\rho_{S_R a} - \rho_{S_R b}) - 2\Gamma_R \rho_{S_R}, \\
\dot{\rho}_+ &= (1-x)\Gamma_L \rho_1 - x\Gamma_L \rho_+, \\
\dot{\rho}_- &= (1-x)\Gamma_L \rho_2 - x\Gamma_L \rho_-,
\end{aligned} \tag{22}$$

for the diagonal elements which describe occupation probabilities and

$$\begin{aligned}
\dot{\rho}_{ab} &= it_{LR}(\rho_{S_R b} + \rho_{aS_R}) - x\Gamma_L \rho_{ab}, \\
\dot{\rho}_{aS_R} &= it_{LR}(\rho_{S_R} - \rho_a + \rho_{ab}) - \left(i\varepsilon + \frac{1}{2}(x\Gamma_L + 2\Gamma_R)\right)\rho_{aS_R} \\
\dot{\rho}_{bS_R} &= -it_{LR}(\rho_{S_R} - \rho_b + \rho_{ba}) - \left(i\varepsilon + \frac{1}{2}(x\Gamma_L + 2\Gamma_R)\right)\rho_{bS_R},
\end{aligned} \tag{23}$$

for the off-diagonal elements, i.e. the coherences, where  $\varepsilon = \varepsilon_L - \varepsilon_R + U_{LR} - U_R$ .

The spin current operators  $\mathcal{J}_{\sigma\pm}$  can be written as matrices for which all elements but  $(\mathcal{J}_{\uparrow+})_{2,S_R} = (\mathcal{J}_{\downarrow+})_{1,S_R} = \Gamma_R$  vanish. Processes which transport an electron from the collector to the state  $|S_R\rangle$  are energetically forbidden and, thus,  $\mathcal{J}_{\sigma-} = 0$ .

Under the condition  $\varepsilon = 0$ , we find that  $|a\rangle$  and  $|b\rangle$  are in resonance with  $|S_R\rangle$  such that for symmetric dot–lead coupling  $\Gamma_L = \Gamma_R = \Gamma$ , a leakage current  $I = xe\Gamma/3$  emerges. Then, the Fano factor is determined by the internal dynamics even in the limit of small thermal excitation  $x \ll 1$  and reads

$$F = \frac{5}{3} - \left(\frac{7}{3} + \frac{4\Gamma^2}{9t_{LR}}\right)x + O(x^2). \tag{24}$$

This super-Poissonian shot noise can be explained in terms of electron bunching: spin blockade occurs once electrons decay to a triplet state. Then, the system will remain for a rather long period in the triplet subspace, intermitted only by short lapses of time in which an electron tunnels to the emitter and is replaced by an electron with opposite spin and, thereby, resolves spin blockade. The resulting electron bunching turns into super-Poissonian statistics, as in the case of dynamical channel blockade [24, 28, 29], where two interacting channels block each other. Here, the two channels are replaced by the two interacting spin degrees of freedom.

Interestingly enough, this result can be compared to the transport through a single quantum dot for which one level (the singlet channel) lies within the transport window and three



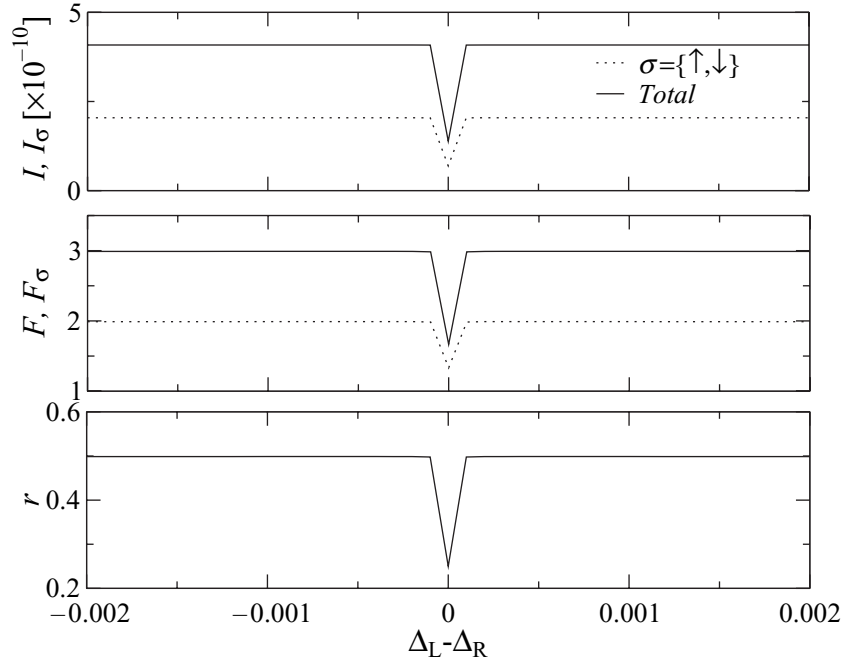


**Figure 3.** Current (in  $\text{mV}/\hbar$ ), Fano factors and spin correlation for the undriven case, as a function of Zeeman inhomogeneity for  $t_{\text{LR}} = 0.0026$ ,  $\varepsilon_{\text{L}} = 1.5$ ,  $\varepsilon_{\text{R}} = 0.45$ ,  $U_{\text{R}} = 1.45$ ,  $\Delta_{\text{R}} = 0.026$  (corresponding to a magnetic field of  $\sim 1\text{T}$ ),  $\mu_{\text{L}} = 1.94$ ,  $\mu_{\text{R}} = 1.1$ ,  $\Gamma_{\text{L}} = \Gamma_{\text{R}} = 10^{-3}$  and  $k_{\text{B}}T = 0.001$  (energies in  $\text{meV}$ ).

levels (the three inter-dot triplets) are below both Fermi surfaces, such that the occupation of the latter states induces dynamical channel blockade. Then the Fano factor becomes  $F = 1 + (4/3)\Gamma_{\text{L}}/(\Gamma_{\text{L}} + \Gamma_{\text{R}})$  and for  $\Gamma_{\text{L}} = \Gamma_{\text{R}}$  assumes the value  $F = 5/3$ .

In the absence of spin scattering processes, both spins contribute equally to the current,  $I_{\sigma} = I/2$ , and the Fano factor for each spin current reads

$$F_{\sigma} = \frac{4}{3} - \left( \frac{7}{6} + \frac{2\Gamma^2}{9t_{\text{LR}}^2} \right) x + O(x^2). \quad (25)$$

Moreover, we obtain the spin correlation coefficient

$$r = \frac{1}{4} - \frac{42\Gamma^2 + 21t_{\text{LR}}^2}{32t_{\text{LR}}^2} x + O(x^2). \quad (26)$$

As can be seen in figure 3, this behaviour considerably changes as soon as an inhomogeneity in the Zeeman splittings appears. Then mixing between  $|S_0\rangle$  and  $|T_0\rangle$  adds a new conducting channel while the number of blocking states is reduced to the two states  $|+\rangle$  and  $|-\rangle$  and, thus, the effective transmitted charge and the Fano factor increase. Then, we find  $F = 3$ ,  $F_{\sigma} = 2$ , and  $r = 1/2$ .

#### 4. Electron spin resonance

The spin of an electron can be manipulated by external magnetic fields. For instance, in the presence of an oscillating magnetic field  $B_{\text{ac}}$  whose frequency equals the Zeeman splitting

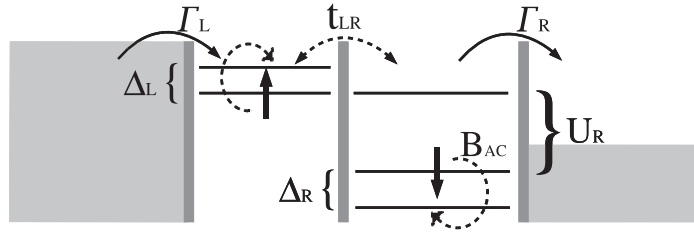


**Figure 4.** Spin rotation in a double quantum dot induced by an oscillating magnetic field at resonance with the Zeeman splitting.

produced by a constant magnetic field, the electron spins rotate, which is known as the electron spin resonance [30]. For quantum dots, this effect may manifest itself in current oscillations [8] and allows one to determine the spin scattering times [31].

In a double quantum dot, one expects that the rotation of a single electron spin removes spin blockade [9], but the presence of a second electron can lead to collective rotations which quench the current or affect the current oscillations [10]. This behaviour is reflected also in the shot noise characteristics, as we will find below.

When a magnetic field with an ac component circularly polarized perpendicular to the  $x$ - $y$ -plane acts, then the  $z$ -components of the electron spins start to rotate, as depicted in figure 4. The corresponding time-dependent Hamiltonian reads

$$\hat{H}_B(t) = \sum_i \left[ \Delta_i \hat{S}_z^i + g B_{ac} \left( \hat{S}_x^i \cos \omega t + \hat{S}_y^i \sin \omega t \right) \right]. \quad (27)$$

In order to rotate the electron spin, the frequency of the ac magnetic field must satisfy the resonance condition  $\hbar\omega = \Delta_i$  [8]. Then one would naively expect that the Pauli exclusion principle eventually would not apply to the interdot tunnelling such that spatial oscillations between the left and right quantum dots occurred and a finite current emerged. For a homogeneous Zeeman splitting through the double dot,  $\Delta_L = \Delta_R$ , however, this is not the case. As the oscillating magnetic field brings different spin projections within one dot into resonance, the electron spins in different quantum dots rotate simultaneously within the triplet subspace, which is decoupled from the singlets. Then, the electrons become eventually trapped in the triplet subspace and the tunnelling current towards the collector drops to zero [10].

The Zeeman splittings in different dots may as well be different,  $\Delta_L \neq \Delta_R$ , for example, due to an inhomogeneous magnetic field  $B_{dc}$ . A further reason may be a dependence of the  $g$ -factors on the particular quantum dot, or a difference in the hyperfine interaction [13, 32]. Then, the states  $|S_0\rangle$  and  $|T_0\rangle$  mix and, thus, only the triplet states  $|+\rangle$  and  $|-\rangle$  suffer from spin blockade. Moreover, since for an inhomogeneous Zeeman splitting,  $B_{ac}$  can only be at resonance with the electrons in one of the quantum dots, the trapping in the triplet subspace is lifted and a finite current can flow; see figure 5.

The contribution of these two effects—single electron spin resonance and the suspension of channel blocking by singlet–triplet mixing—results in a non-monotonic dependence of the Fano factor, which is considerably enhanced in the vicinity of the degenerate Zeeman splitting  $\Delta_L \approx \Delta_R$ . In that region, the rotation of the two electrons still dominates and increases the blocking time which is much longer than the time lapses with finite conduction. This leads to an enhanced electron bunching which is manifest in the larger Fano factor shown in figure 5.

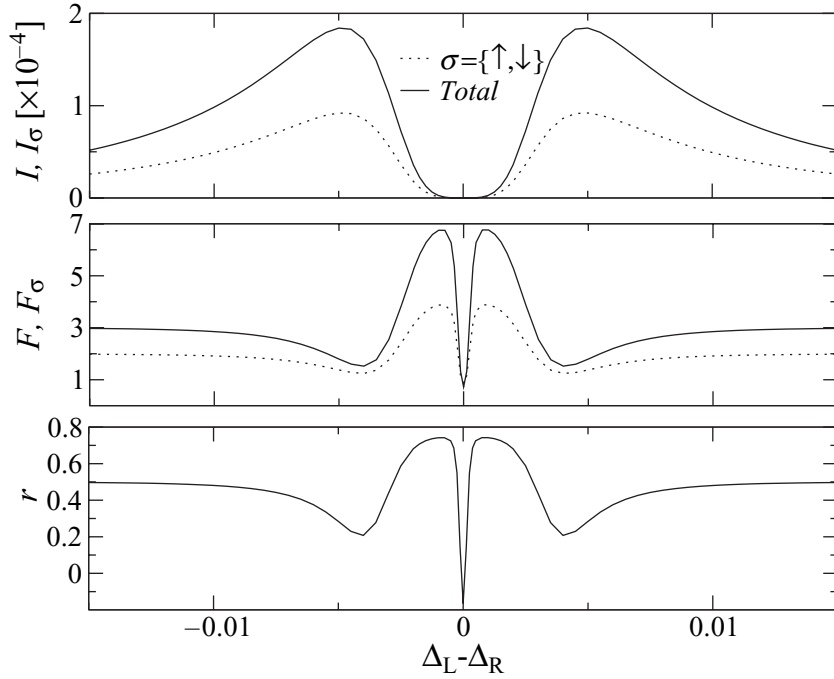


**Figure 5.** Current (in  $\text{mV}/\hbar$ ), Fano factors, and spin correlation as a function of the Zeeman inhomogeneity for magnetic field intensity  $B_{\text{ac}} = 0.1\sqrt{2}\text{T}$ ,  $t_{\text{LR}} = 0.0026$ ,  $\varepsilon_{\text{L}} = 1.5$ ,  $\varepsilon_{\text{R}} = 0.45$ ,  $U_{\text{R}} = 1.45$ ,  $\hbar\omega = \Delta_{\text{R}} = 0.026$ ,  $\mu_{\text{L}} = 2$ ,  $\mu_{\text{R}} = 1.1$ ,  $\Gamma_{\text{L}} = \Gamma_{\text{R}} = 10^{-3}$  and  $g = 0.026$  (energies in meV).

This super-Poissonian behaviour is accompanied by an enhanced spin correlation coefficient  $r$ . Once single-electron spin resonance dominates owing to large Zeeman inhomogeneities, the Fano factors of both the charge current and the spin current saturate at the values  $F = 3$  and  $F_{\sigma} = 2$ , respectively, whereas the spin correlation coefficient becomes  $r = 1/2$ .

#### 4.1. Crossover to the incoherent regime: unblocking by relaxation

The presence of inelastic spin scattering processes damps the coherent rotations within the triplet subspace resulting in a finite population of the singlet subspace. Then, a finite current emerges. We treat relaxation processes phenomenologically by introducing in the master equation spin relaxation and spin dephasing times,  $T_1$  and  $T_2$ , respectively.

The results for the Fano factors and the spin correlation for  $\Delta_{\text{L}} = \Delta_{\text{R}}$  shown in figure 6 indicate the existence of two different regimes: when spin relaxation processes represent merely a perturbation, only a small leakage current flows and the Fano factors approach  $F = 5/3$  and  $F_{\sigma} = 4/3$ , whereas the spin correlation coefficient becomes  $r = 1/4$ . As spin relaxation becomes more important, the current increases to a maximum which marks the crossover to the incoherent regime. At the maximum, the current and the spin current are sub-Poissonian,  $F, F_{\sigma} < 1$ . For even faster relaxation processes, typically for  $T_1 < 2\pi/\Omega_{\text{ac}}$ , both spin rotation and inter-dot tunnelling—which are considered to be of the same order here, with Rabi frequencies  $\Omega_{\text{ac}} = 2B_{\text{ac}}$  and  $\Omega_{\text{LR}} = 2\sqrt{2}t_{\text{LR}}$  [10]—are no longer effective, so that spin relaxation takes place immediately after spin rotation. Consequently, no electron flow is observed [10].

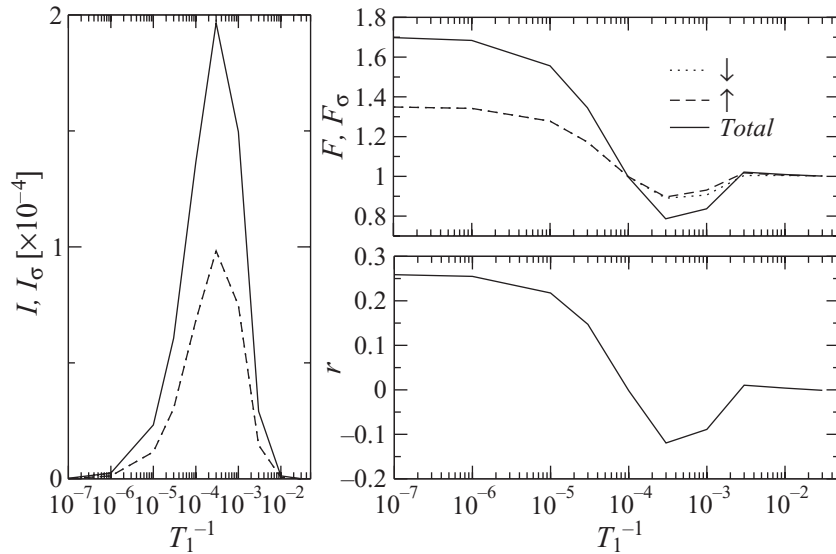


**Figure 6.** Current (in  $\text{mV}/\hbar$ ), Fano factors and spin correlation as a function of the spin relaxation rate. We have considered  $T_2 = 0.1T_1$  and the same parameters as in figure 5, except for  $\Delta_L = \Delta_R = 0.026$ .

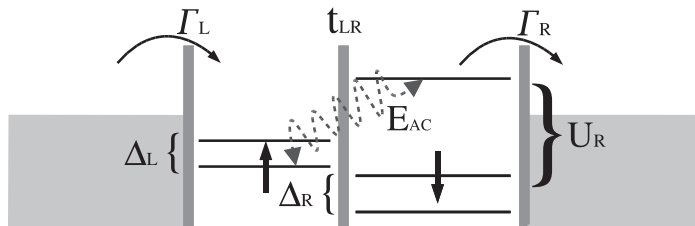


**Figure 7.** Pumping configuration, where spin blockade is removed by photon-assisted processes through the contact barriers.

As expected, in this regime the currents are almost Poissonian and the spin projections are uncorrelated.

## 5. Pumping and photon-assisted transport

Not only an ac-magnetic field, but also an ac-electric field can support the electron transport by exciting electrons to states which lie above the chemical potentials of both leads and, thus, are energetically forbidden. Then, the triplet states have finite lifetimes due to photon absorption processes so that spin blockade is resolved [1, 33]. A paradigmatic setup for which resonant ac-electric fields can lead to finite charge [34] or spin currents [16] even in the absence of a source–drain voltage ( $\mu_L = \mu_R = \mu$ ) is the spatially asymmetric *pump* configuration of the double dots sketched in figure 7. There the asymmetry is provided by the different intra-dot interactions  $U_L > U_R$ . Pumping occurs when the frequency of the electric ac-field provides the energy necessary to transfer the electron from the left quantum dot to an energetically higher singlet state  $|S_R\rangle$  in the right dot. For this process, the resonance condition reads  $\hbar\omega = \hbar\omega_0 = \varepsilon_R - \varepsilon_L + U_R - U_{LR}$ . As before, the singly occupied states of both dots are below both

chemical potentials,  $\varepsilon_l < \mu$ , whereas the doubly occupied singlets lie well above,  $U_l + \varepsilon_l > \mu$ . We restrict ourselves to the pumping configuration, because increasing the bias voltage reduces the contribution of photon assisted processes through the contact barriers [35, 36] that are essential for removing the spin blockade.

The ac-electric field is modelled as an oscillatory dipole potential, i.e. as a time-dependent energy shift with a phase  $\pi$  between the two dots. Then the Hamiltonian (1) acquires a term

$$\hat{H}_{\text{ac}}(t) = \frac{eV_{\text{ac}}}{2} (\hat{n}_{\text{L}} - \hat{n}_{\text{R}}) \cos(\omega t). \quad (28)$$

By the unitary transformation  $\hat{U}(t) = e^{i(eV_{\text{ac}}/2\hbar\omega)(\hat{n}_{\text{L}} - \hat{n}_{\text{R}}) \sin \omega t}$ , the time dependence is transferred to the tunnel couplings according to

$$\hat{H}'(t) = \hat{U}(t) \left( \hat{H} - i\hbar \partial_t \right) \hat{U}^\dagger(t) = \hat{H}_0 + \hat{H}'_{\text{LR}}(t) + \hat{H}'_{\text{T}}(t) + \hat{H}_{\text{leads}}, \quad (29)$$

where

$$\hat{H}'_{\text{LR}}(t) = \sum_{\nu=-\infty}^{\infty} (-1)^\nu J_\nu \left( \frac{eV_{\text{ac}}}{\hbar\omega} \right) \sum_{\sigma} \left( t_{\text{LR}} e^{i\nu\omega t} \hat{c}_{\text{L}\sigma}^\dagger \hat{c}_{\text{R}\sigma} + \text{h.c.} \right), \quad (30)$$

$$\hat{H}'_{\text{T}}(t) = \sum_{\nu=-\infty}^{\infty} (-1)^\nu J_\nu \left( \frac{eV_{\text{ac}}}{2\hbar\omega} \right) \sum_{lk\sigma} \left( \gamma_l e^{i\nu\omega t} \hat{d}_{lk\sigma}^\dagger \hat{c}_{l\sigma} + \text{h.c.} \right). \quad (31)$$

Thus the driving effectively renormalizes the inter-dot tunnelling by the Bessel function  $J_\nu$ , where the index  $\nu$  reflects the number of photons involved. This creates dynamical charge localization under conditions that we specify below. The corresponding photon-assisted tunnelling rates turn out to be

$$\Gamma_{mn} = \frac{2\pi}{\hbar} \sum_{l\nu} d_l J_\nu^2 \left( \frac{eV_{\text{ac}}}{2\hbar\omega} \right) |\gamma_l|^2 (1 - f_l(\hbar\omega_{mn} + \nu\hbar\omega)), \quad (32)$$

$$\Gamma_{mn} = \frac{2\pi}{\hbar} \sum_{l\nu} d_l J_\nu^2 \left( \frac{eV_{\text{ac}}}{2\hbar\omega} \right) |\gamma_l|^2 f_l(\hbar\omega_{mn} + \nu\hbar\omega), \quad (33)$$

where the former rate governs processes  $|n\rangle \rightarrow |m\rangle$  that remove an electron from the double dot, whereas the latter refers to adding an electron to the system. The density of states in the leads,  $d_l$ , is assumed to be constant.

If a magnetic field is applied such that the energies of the spin-down electrons are shifted by  $\Delta_l$ , the spin-up electron is delocalized within the double quantum dot occupying the states  $|\uparrow, \downarrow\rangle$  and  $|0, \uparrow\downarrow\rangle$  until one of the electrons tunnels to the right lead. If the Zeeman splitting is the same in both dots, the spin-down electron can at the same time be delocalized between  $|0, S_{\text{R}}\rangle$  and  $|\downarrow, \uparrow\rangle$  for the same frequency.

At low ac intensities, photon-assisted tunnelling is not significant. Indeed, using the approximation  $J_\nu(x) \approx \delta_{\nu,0}$  for small  $x$ , we find that photon-assisted tunnelling rates become identical to the rates for the static system discussed in section 3; cf figure 8. When increasing the intensity, both the current and the noise exhibit a more involved behaviour stemming from the amplitude and frequency dependence of the tunnel rates via the arguments of the Bessel functions  $J_1(eV_{\text{ac}}/\hbar\omega)$  and  $J_1(eV_{\text{ac}}/2\hbar\omega)$  that govern inter-dot tunnelling and photon-assisted

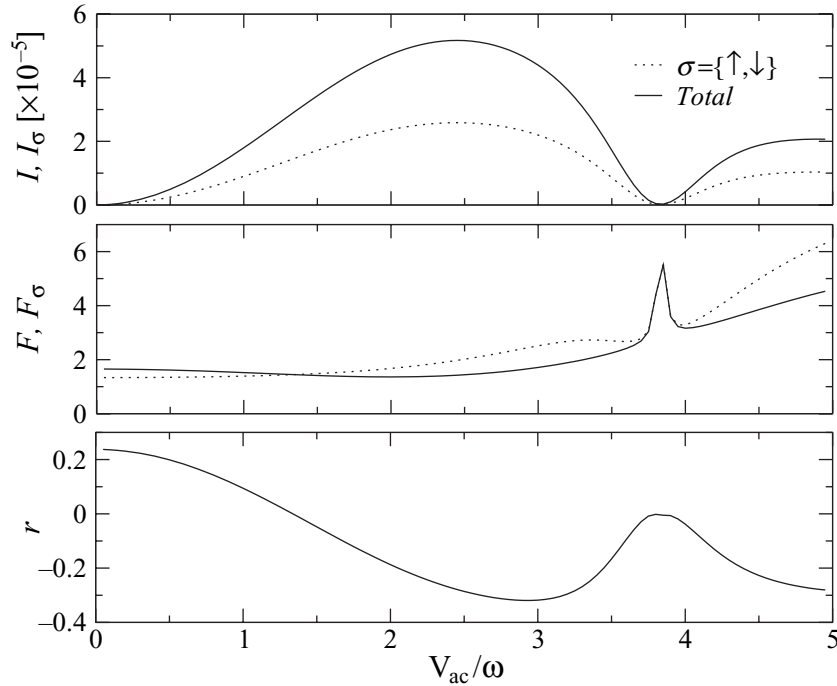


**Figure 8.** Current (in  $\text{mV}/\hbar$ ), Fano factors and spin correlation as a function of the electric field intensity for  $\omega = \omega_0$ ,  $t_{\text{LR}} = 0.005$ ,  $\varepsilon_{\text{L}} = 0.4$ ,  $\varepsilon_{\text{R}} = 0.25$ ,  $U_{\text{R}} = 1$ ,  $U_{\text{LR}} = 0.5$ ,  $\Delta_{\text{L}} = \Delta_{\text{R}} = 0.026$ ,  $\mu_{\text{L}} = \mu_{\text{R}} = 1.2$  and  $\Gamma_{\text{L}} = \Gamma_{\text{R}} = 10^{-3}$  (energies in  $\text{meV}$ ).

tunnelling, respectively. When the ac-intensity approaches the value for which  $J_1(eV_{\text{ac}}/\hbar\omega)$  assumes its maximum, inter-dot tunnelling is most effective and, thus, the current assumes its maximum as well, whereas the Fano factor assumes a minimum [37]. The spin Fano factor, by contrast, does not assume a minimum and, consequently, the spin correlation  $r$  becomes negative. Increasing the ac-intensity further reduces the net current because in this limit, the rates of left-to-right tunnelling approach those of the opposite processes. This cancellation does not affect the noise strength  $S$ , so that a smaller current leads to an increasing Fano factor.

Particularly interesting is the condition  $J_1(eV_{\text{ac}}/\hbar\omega) = 0$  for which dynamical charge localization is found. Then one-photon interdot tunnelling is suppressed due to the renormalization factor in the hopping term (30). Since for our configuration these processes represent the main contribution to the transport, the current becomes strongly suppressed, as can be appreciated in figure 8 in the region close to  $eV_{\text{ac}} \approx 3.8\hbar\omega$ . Nevertheless, photon-assisted tunnelling through the contacts is still noticeable by its contribution to the current fluctuations, leading to a sharp peak in the Fano factor [38]. This behaviour is different from the one found in the large bias limit, where current suppression is associated with Poissonian noise [39].

Another important factor for spin blockade is the difference between the Zeeman splittings, as discussed in section 4. If  $\Delta_{\text{L}} = \Delta_{\text{R}}$ , the states  $|\uparrow, \downarrow\rangle$  and  $|\downarrow, \uparrow\rangle$  are indistinguishable, then the inter-dot singlet  $|S_0\rangle$  and the triplet  $|T_0\rangle$  influence the dynamics. Since inter-dot tunnelling does not change the total spin, it can only occur within the singlet states  $|S_0\rangle$  and  $|S_{\text{R}}\rangle$ . Thus, not only the states  $|\uparrow, \uparrow\rangle$  and  $|\downarrow, \downarrow\rangle$  contribute to the transport blocking, but also the triplet state  $|T_0\rangle$ .

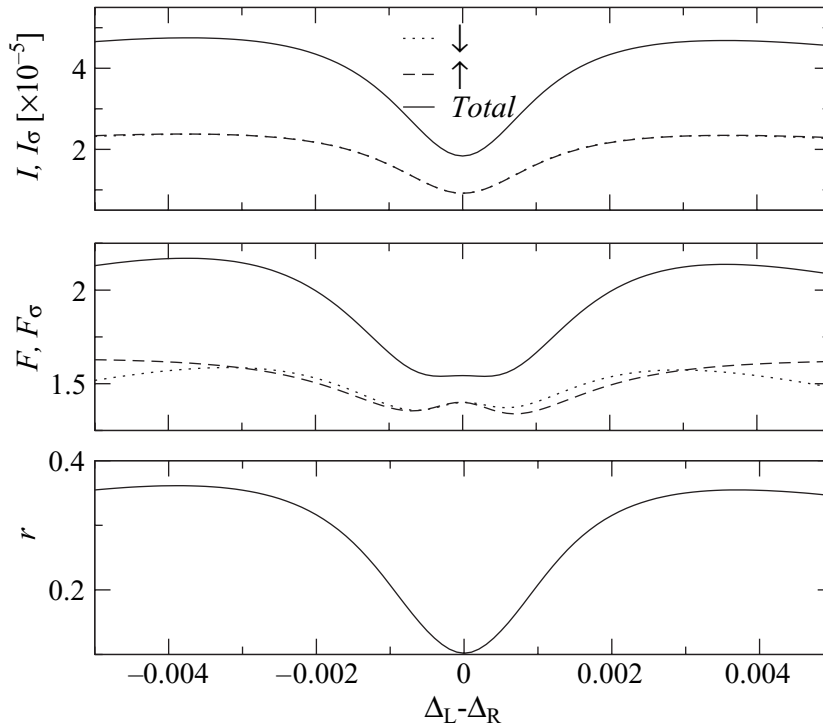


**Figure 9.** Current, Fano factor and spin correlation as functions of the Zeeman inhomogeneity (by varying  $\Delta_L$ ) for  $eV_{ac} = \hbar\omega = \hbar\omega_0$  and the same parameters as in figure 8. Though the spin currents almost coincide, as seen in the upper panel, their dynamics can be distinguished in the noise components.

On the other hand, if the Zeeman splittings are different,  $\Delta_L \neq \Delta_R$ , spin blockade is less effective due to the mixing between the states  $|T_0\rangle$  and  $|S_0\rangle$  [10]. Then the current increases, as can be seen in figure 9. The reduced number of blocking states again diminishes the Fano factor. If the difference between the Zeeman splittings is large enough, we find resonant one-photon inter-dot tunnelling for electrons with one particular spin-polarization—here the spin-up polarization. Consequently, the transport becomes spin-dependent, as can be appreciated in the different Fano factors in figure 9.

## 6. Conclusions

In this work, we have studied the suspension of spin blockade in the electron transport through coherently coupled double quantum dots by ac-driving fields, thermal excitations and spin-flip scattering. In particular, we focused on the associated shot noise characterized by the Fano factors for the electron and the spin currents, as well as on the spin–spin correlation coefficient.

One way to resolve spin blockade is the application of magnetic fields that cause Zeeman splitting or spin rotation. Most interestingly, we found that the current noise for both charge transport and spin transport depends sensitively on whether the Zeeman splitting is the same or different for the two dots. For degenerate Zeeman splitting, the eigenstates are delocalized and the transport across the whole sample is dominated by tunnel events which obey Poissonian statistics. Thus the Fano factors tend to be close to unity. If the degeneracy is absent, transport

is dominated by lapses of time in which spin blockade is lifted. During these lapses, we observe the transport of bunches of electrons with correlated spins.

Considering also spin relaxation, we find that such incoherent processes can even contribute to the suspension of the spin blockade: with an increasing relaxation rate, transport is enhanced and becomes more regular and even sub-Poissonian. When the predominantly incoherent regime is entered, the Fano factor increases again until we eventually reach an incoherent regime with Poissonian tunnel currents.

Time-dependent fields can also resonantly excite electrons to orbitals with energies above both Fermi surfaces. In that way, they may cause photon-assisted transport and, in asymmetric configurations, electron pumping. The latter results in a contribution to the dc-current at zero bias voltage. Photon-assisted transport can be described by performing a unitary transformation of the Hamiltonian such that only the tunnelling matrix elements are explicitly time-dependent. This renormalizes the tunnel couplings such that they depend on driving amplitude and frequency. The main contribution to inter-dot hopping can even vanish, so that for specific driving parameters, the electrons become localized within one dot. Consequently, the current is almost suppressed. Nevertheless, the current fluctuations may stay at a significant level and, accordingly, the shot noise level is super-Poissonian. With an additional Zeeman splitting, the resonance condition becomes spin-dependent. Then photon-assisted transport favours one particular spin projection and the two spin currents are no longer identical. This also affects the spin shot noise, although the difference in the corresponding Fano factors turns out to be relatively small.

In conclusion, our results underline that ac-fields can have intriguing consequences for spin-dependent transport. Depending on the type of excitation, both charge transport and spin transport can occur in bunches. We have shown that this should be clearly visible in the corresponding measurements of the Fano factor and, most likely, also in higher orders of the full-counting statistics. For driven spin transport this still is awaiting closer investigation.

## Acknowledgments

Work supported by the MEC of Spain through grant no. MAT2005-00644. SK acknowledges support by the DFG through SFB 484 and the Excellence Cluster ‘Nanosystems Initiative Munich (NIM)’.

## References

- [1] Hanson R, Kouwenhoven L P, Petta J R, Tarucha S and Vandersypen L M K 2007 *Rev. Mod. Phys.* **79** 1217
- [2] Großmann F, Dittrich T, Jung P and Hänggi P 1991 *Phys. Rev. Lett.* **67** 516
- [3] Großmann F and Hänggi P 1992 *Europhys. Lett.* **18** 571
- [4] Platero G and Aguado R 2004 *Phys. Rep.* **395** 1
- [5] Kohler S, Lehmann J and Hänggi P 2005 *Phys. Rep.* **406** 379
- [6] Della Valle G, Ornigotti M, Cianci E, Foglietti V, Laporta P and Longhi S 2007 *Phys. Rev. Lett.* **98** 263601
- [7] Brandes T, Aguado R and Platero G 2004 *Phys. Rev. B* **69** 205326
- [8] Engel H-A and Loss D 2002 *Phys. Rev. B* **65** 195321
- [9] Koppens F H L, Buizert C, Tielrooij K J, Vink I T, Nowack K C, Meunier T, Kouwenhoven L P and Vandersypen L M K 2006 *Nature* **442** 766
- [10] Sánchez R, López-Monís C and Platero G 2008 *Phys. Rev. B* **77** 165312



- [11] Weinmann D, Häusler W and Kramer B 1995 *Phys. Rev. Lett.* **74** 984
- [12] Ono K, Austing D G, Tokura Y and Tarucha S 2002 *Science* **297** 1313
- [13] Iñarrea J, Platero G and MacDonald A H 2007 *Phys. Rev. B* **76** 085329
- [14] Fransson J and Råsander M 2006 *Phys. Rev. B* **73** 205333
- [15] Cota E, Aguado R, Creffield C E and Platero G 2003 *Nanotechnology* **14** 152
- [16] Sánchez R, Cota E, Aguado R and Platero G 2006 *Phys. Rev. B* **74** 035326
- [17] Creffield C E and Platero G 2002 *Phys. Rev. B* **65** 113304
- [18] Flindt C, Novotny T and Jauho A-P 2004 *Phys. Rev. B* **70** 205334
- [19] Kaiser F J and Kohler S 2007 *Ann. Phys.* **16** 702
- [20] Blanter Ya M and Büttiker M 2000 *Phys. Rep.* **336** 1
- [21] Levitov L S and Lesovik G B 1993 *Pis. Zh. Eksp. Teor. Fiz.* **58** 225
- [22] Bagrets D A and Nazarov Yu V 2003 *Phys. Rev. B* **67** 85316
- [23] Flindt C, Novotný T, Braggio A, Sasseti M and Jauho A P 2008 *Phys. Rev. Lett.* **100** 150601
- [24] Belzig W 2005 *Phys. Rev. B* **71** 161301
- [25] Saito K and Eto M 2008 *Physica E* **40** 1149
- [26] Weymann I 2008 *Phys. Rev. B* **78** 045310
- [27] Blum K 1996 *Density Matrix Theory and Applications* (New York: Plenum)
- [28] Sánchez R, Platero G and Brandes T 2007 *Phys. Rev. Lett.* **98** 146805
- [29] Sánchez R, Kohler S, Hänggi P and Platero G 2008 *Phys. Rev. B* **77** 035409
- [30] Cohen-Tannoudji C, Diu B and Lalöe F 1977 *Quantum Mechanics* (New York: Wiley)
- [31] Dong B, Cui H L and Lei X L 2005 *Phys. Rev. Lett.* **94** 066601
- [32] Jouravlev O N and Nazarov Y V 2006 *Phys. Rev. Lett.* **96** 176804
- [33] Sánchez R, Platero G, Aguado R and Cota E 2006 *Phys. Status Solidi b* **243** 3932
- [34] Stafford S A and Wingreen N S 1996 *Phys. Rev. Lett.* **76** 1916
- [35] Stoof T H and Nazarov Yu V 1996 *Phys. Rev. B* **53** 1050
- [36] Sánchez R and Platero G 2007 *Mathematics in Industry* ed L L Bonilla, M A Moscoso, G Platero and J M Vega (Berlin: Springer)
- [37] Strass M, Hänggi P and Kohler S 2005 *Phys. Rev. Lett.* **95** 130601
- [38] Sánchez R, Kaiser F J, Kohler S, Hänggi P and Platero G 2008 *Physica E* **40** 1276
- [39] Camalet S, Lehmann J, Kohler S and Hänggi P 2004 *Phys. Rev. Lett.* **90** 210602